Carderock Division
Naval Surface Warfare Center
Bethesda, Maryland 20084-5000

CDNSWC/TR-61-95-17 July 1995

Metals Department
Research and Development Report

Strength and Crack Resistance Behavior of Mismatched Welded Joints

by
R.L. Tregoning

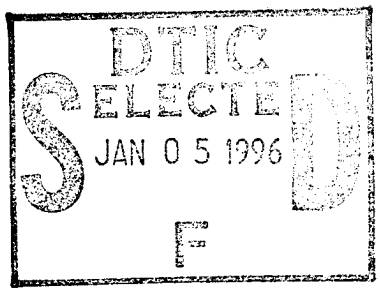

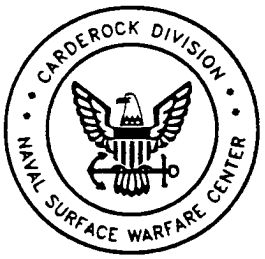

Carderock Division
Naval Surface Warfare Center
Bethesda, Maryland 20084-5000

CDNSWC/TR-61-95-17 July 1995
Metals Department
Research and Development Report

Strength and Cracking Resistance Behavior of Mismatched Welded Joints

by
R.L. Tregoning

TABLE OF CONTENTS

LIST OF FIGURES

LIST OF TABLES

ABSTRACT

A mismatched welded component exists when the strength of the weld material is different than the strength of the base material. This research has examined the effect of weld joint geometry and mismatch level on the strength and fracture performance of high strength steel weld components. Fracture performance was studied only for applied three-point bending loading. Eleven different welded systems were constructed with mismatch ranging between -36% to +47% and various weld joint profiles to sculpt fusion zone widths between 2 and 13 mm at the crack tip. Instrumented tensile tests were utilized to characterize weldment strength behavior while single edge notch bend J-R curve testing of short (a/W = 0.15) and deeply (a/W = 0.5) cracked specimens was conducted to measure both baseline weld metal toughness properties and determine the fracture performance of mismatched systems. The results indicate that contact strengthening in unflawed specimens occurs to a greater degree and at lower constraint in conventional undermatched weldments. Flawed undermatched performance under bending loads is highly dependent on the fusion zone width as well while the degree of mismatching is a secondary effect. As the zone width decreases, the apparent tearing resistance also decreases. The overall performance of undermatched systems, however, can still be better than overmatched systems when the inherent toughness of the overmatching weld metal consumable is poor.

ADMINISTRATIVE INFORMATION

This report was prepared as part of the Ship and Submarine Materials Technology Program sponsored by ONR 332 (Dr. Lewis Sloter). Mr. Ivan Caplan of the Carderock Division, Naval Surface Warfare Center (CDNSWC Code 0115) is the Technology Area Manager for this program. This effort was performed by the Fatigue and Fracture Branch, CDNSWC Code 614 under Program Element 62234N, Structural Alloys Project RS34S55, Work Unit 1-614-554, and was supervised by the Branch Head, Mr. Thomas W. Montemarano.

ACKNOWLEDGEMENTS

The support of Mr. Jack Saveleski and Mr. Joseph Waskey during the initial phase of this research is appreciated. The support of Mr. Robert Meiklejohn, who conducted the majority of the tests presented herein, was crucial. He is also commended for keeping the program and testing schedule on track. Ms. Amber Golshani conducted most of the digital crack length measurements necessary for analysis and her contributions were most helpful and timely. Finally, the support and many helpful discussions of Dr. Richard Link is appreciated. He contributed the initial computer programs for J-R curve analysis and provided much insight into the results and cracking behavior.

INTRODUCTION

Motivation for Mismatched Welding

Currently, naval steels are welded such that the nominal yield strength of the consumable is at least 10% higher than the base metal. This practice is called overmatched welding and resulted in large part from explosion bulge tests conducted in the early 1950s [1,2]. Traditionally, overmatching has been utilized to shield the weld metal from plastic deformation by shedding load to the surrounding base plate material. This practice has been utilized to take advantage of the typically superior and more consistent fracture performance of the base plate material and to decrease the likelihood of failure at an undetected weld defect.

For high strength steel baseplate materials (yield strength, σ_{ys}, > 700 MPa), however, the overmatching philosophy is difficult to employ because there are problems associated with the welding consumables (σ_{ys} > 700 MPa). The inherent toughness of high strength consumables is low and they are also difficult to fabricate because stringent precautions are required to resist hydrogen cracking [3]. Large preheat and interpass temperatures are necessary along with high heat input rates to decrease the weld metal cooling rate [3]. All these precautions decrease welding productivity.

Undermatched welding is the practice of welding a lower strength consumable to the baseplate material. Lower strength welding consumables are desirable because they have better toughness and are easier to fabricate than high strength consumables. However, the primary disadvantage with an undermatched system is that plasticity can be concentrated in the weld during high deformation events. Therefore, welds in overmatched systems undergo

less deformation than undermatched systems but their properties (toughness and ductility) are worse while welds in undermatched systems have better properties, but see concentrated loading. This quandary leads to two important questions which are the focus of this study. Do undermatched high strength steel weldments perform better than overmatched weldments? If not, is the performance of undermatched systems adequate so that the productivity and property gains associated with lower strength consumables can still be realized?

Background

Weldment Performance of Unflawed Specimens -- The effect of mismatching welding on unflawed component performance has been studied quite extensively for tension loading applied transverse to the welding direction [4-9]. For this loading, there is no increase in component strength or ductility for overmatched weldments because the baseplate deformation governs component behavior as long as the weld is free of defects [4]. The strength and ductility for undermatched specimens under tensile loading, however, can be significantly different than for a homogeneous base metal specimen and is a function primarily of the degree of undermatch (i.e. the differences between the base and weld metal yield strengths, strain hardening characteristics, and ultimate strengths, σ_{ult}) and the amount of weld metal constraint [5-9].

Weld metal constraint is typically expressed in terms of a ratio of the weld joint to specimen geometry [6-9]. As this ratio decreases, the weld metal constraint increases and the weldment strength approaches the base metal strength while the failure ductility decreases [6]. This phenomenon is called contact strengthening. As the weld metal constraint decreases, the

weldment tensile properties approach those of the weld metal.

Weldment Performance of Flawed Specimens -- Analytical and numerical studies have characterized the behavior of flawed, mismatched components also as a function of mismatch level, constraint, and deformation level. As the crack length (a) becomes large compared to the remaining ligament (b) and weld zone height (L_{hgt} in Fig. 1), the applied J approaches the solution for the homogeneous baseplate material [10,11]. Conversely, when the crack length is large and the weld joint height is much greater then the remaining ligament, the weldment response is similar to a solely weld metal specimen [10]. The bulk of structurally relevant applications, however, falls between these two extremes when fusion line interferes with the crack tip plastic zone and alters the crack tip driving force. In these cases, overmatching shields the crack tip and the applied J decreases. Undermatching concentrates deformation and the applied J compared to a homogeneous specimen. Orders of magnitude differences in applied J appear to be possible for moderate amounts of mismatch (±10%) depending on the deformation level, loading mode, specimen and crack geometry, and joint geometry [12-14].

Experimental determination of flawed mismatched weldment behavior is complicated by the fact that the J-integral loses path independency for mismatched weld joints when the contour crosses the fusion line [10] except in special cases [15]. J-integral computations are only accurate when the contour is contained locally within the weld [10,13]. Therefore, current experimental procedures to determine the weldment J-R behavior are not rigorously accurate since they require remote measurements to calculate J. Kirk, however, has shown that for single edge notched bend [SE(B)] specimens, J-integral determination based on

standard experimental techniques [16] is accurate to within 10% of the actual J for a variety of weld joint geometries, mismatch levels of ±20%, and for J deformation levels up to 350 kJ/m^2 [10].

APPROACH

Naval high strength structural steels and welding consumables were utilized to create a number (eleven) of overmatched and undermatched weldment systems with varying weld joint geometries. Mismatch ratios were varied simply by welding high and low strength consumables into each baseplate material using standard procedures. These mismatch levels are representative of potential structural applications. The weld joint geometries were also chosen to represent a range of possible production welds.

Additional care was taken to ensure that the flawed weldment performance was influenced by mismatching to the greatest extent possible. This was ensured with the aid of Fig. 2 [10] which illustrates how the weldment crack driving force (J_{wj}) for a specimen under three-point bend loading compares to the applied J in a homogeneous weld specimen (J_{aw}) as a function of L_{min}/a: L_{min} is the distance between the weld joint fusion line and a is the crack length. The weldment crack driving force is nearly equivalent to the homogeneous driving force as $L_{min}/a \rightarrow 0$ and $L_{min}/a \gtrsim 3$ which represent the deep and short crack limits discussed earlier. The weldment applied J is influenced to the largest extent between these two extremes. Weld joint geometries were chosen so that fracture performance would be measured near the long and short crack limit and in the intermediate region to maximize mismatch effects.

The strength and toughness of each baseplate and weld consumable which produced the weldments were characterized using conventional Charpy and tensile testing. Then, instrumented transverse tensile tests were utilized to determine if performance degradation was evident in the undermatched weldment systems compared to the homogeneous weld and base metal properties. Next, the baseline cracking resistance (J-R) of the weld metal was measured using deeply flawed (a/W = 0.5) SE(B) specimens with $L_{min}/a < 1$ to minimize mismatch effects. The effect of weld joint geometry and mismatch ratio on the cracking resistance was then studied using short crack (a/W = 0.15) SE(B) specimens with a wide range of L_{min}/a ratios.

MATERIAL AND WELDMENT PREPARATION

Two common naval structural steels were utilized as the baseplate materials for the weldments: HY-80 and HY-100. HY-80 and HY-100 have nominal yield strengths of 550 MPa and 690 MPa respectively. Three welding consumables were used as weld filler material: Mil-70S, Mil-100S, and Mil-120S. These consumables have nominal maximum yield strengths of approximately 480 MPa, 690 MPa, and 830 MPa respectively. The specified chemical compositions for these materials are summarized in Table 1 and were obtained from [17] for the weld metal filler and [18] for the base steels. Maximum values are reported in this table unless a range is given.

Eleven different butt weldments were manufactured in 50 mm thick baseplate through permutations in the choice of welding consumable, baseplate, and weld joint geometry. A schematic of the relevant weld joint profile characteristics is illustrated in Fig. 3 along with a

summary of the specific geometry for each of the eleven weldments. In this summary, the baseplate material and weld filler material is listed for each weldment along with three geometric parameters necessary to uniquely describe each joint design: the minimum gap width, L_{gap}, the height of the root, L_{rht}, and the included angle of the weld, θ_{inc}. These variables are related and can be used to determine L_{min} as defined in Fig. 2.

All weldments were produced using gas metal arc welding (GMAW) with M-2 (2% oxygen, 98% argon) shielding gas. The preheat temperature and interpass temperature range were 120°C and 120-135°C respectively. The heat input was 2.16 kJ/mm. The parameters were constant for every weld and were chosen so that the weld metal cooling was three-dimensional [19]. This practice was employed in an attempt to achieve consistent weld metal properties regardless of the joint design. However, these welding parameters also fall well within the allowable ranges for production welds [20].

EXPERIMENTAL PROCEDURES

Baseplate and Weld Metal Characterization

Tensile testing was conducted on the baseplate and all-weld metal specimens at -2°C to concur with subsequent J-R curve testing. Triplicate specimens were tested as per ASTM E8 [21]. The baseplate and all-weld specimen orientation was "L" where, for the all-weld specimens, "L" is defined as the welding axis. All-weld specimens were not tested from every weldment; rather, a few representative weldments were tested to provide an indication of the variability among a each weld consumable between different weldments. The weldments used to characterize the all-weld metal specimens are indicated in Table 2.

Charpy V-notch testing of all-weld specimens was conducted as per ASTM E23 [22] to determine the ductile to brittle transition behavior of some representative samples for each welding consumable. The specimen orientation was T-S. At a minimum, triplicate specimens were tested for each upper and lower shelf temperature while five specimens were utilized in the transition regime. The weldments utilized for this testing are indicated in Fig. 4. All other welds were tested at a single upper and lower shelf temperature so that a comparison could be made among welds with the same consumable. Charpy toughness comparisons were avoided within the transition range due to the additional variability inherent in this region.

Weldment Tensile Testing

The weldment strength testing was conducted using specimens oriented transverse (T) to the weld axis and plate rolling direction. Standard round 12.8 mm diameter tensile specimens [21] were machined with the weld metal located in the center of the specimen gage length (Fig. 5). Separate strain gages were positioned solely in the baseplate and weld metal regions. An extensometer with a 50 mm gage length was also employed to span the weld region and record the composite specimen response (Fig. 5). Testing was conducted at -2°C. All testing procedures and analysis were conducted in accordance with ASTM E8 [21].

Weldment tensile testing was performed for selected undermatched systems (GXK, GXP, GXR, GXS, and GXT). As mentioned, overmatched specimen behavior follows the homogeneous baseplate response. For the symmetric double-V weldments (GXP, GXR, and GXT), triplicate specimens were tested from the center of the plate to coincide with the weld

root pass where the weld joint height is the minimum. The asymmetric double-V (GXK) and single-V (GXS) weldments had triplicate specimens taken from the top and bottom of the plate to sample two unique weld joint heights within the same weld.

J-R Curve Testing and Analysis

Specimens and Test Conditions -- The crack growth resistance behavior under applied bending loads was measured in the T-S orientation with respect to the weld. The crack was located along the weld centerline as in Fig. 3. Standard 1T SE(B) specimens [16] were side grooved with a 10% thickness reduction on each side and used for this testing. The starter notch for each specimen was manufactured using electric discharge machining (EDM). The notch width was 0.5 mm and the notch tip radius was 0.25 mm. Once again, testing was conducted at -2°C and triplicate specimens were utilized for each unique condition except for some short crack specimens as noted.

Deep crack toughness testing (a/W = 0.5) was performed to measure the baseline weld metal cracking resistance for each consumable. HY-80 baseplate weldments GXK (Mil-70S), GXL (Mil-100S), and GXM (Mil-120S) were chosen for this testing. The average L_{gap}/a ratio for the deep crack weldments was 0.5 for GXK, 0.2 for GXL, and 0.7 for GXM. Short crack testing (a/W = 0.15) was conducted for a variety of L_{gap}/a ratios for the remainder of the weldments. Figure 3 summarizes the nominal L_{gap}/a ratio for each weldment system. Triplicate specimens were utilized except for the large gap GXM and small gap GXN configurations where only two specimens were tested and for the large gap GXU configuration which is represented by only one specimen.

Testing Technique -- Prior to testing, the specimens were loaded in nearly three-point compression to 50% of the limit load for one cycle. Precompression was employed to homogenize the residual stress distribution around the crack tip throughout the specimen thickness. This procedure was necessary to generate straight crack fronts during fatigue precracking and also to minimize the effect of residual stresses on the R-curve [23]. This method consistently led to straight crack fronts as evidenced in Fig. 6.

The crack resistance curves were measured in accordance with the requirements of the draft Standard Method for Fracture Toughness Testing[1] where applicable. A single specimen, computer interactive, unloading compliance method was utilized to monitor the applied J-integral and crack length during the test. Unloading compliance is a viable technique for crack length measurement down to a/W = 0.1 [24]. The necessary short crack compliance expression is documented in [25] and is valid between $0.05 <= a/W <= 0.45$. The standard compliance expression presented in ASTM E1152 [16] was adequate for the deeply crack specimens. Load line displacement was measured with a flex bar attached directly to the specimen to avoid errors that can occur from specimen brinelling.

Applied J Determination -- The applied J values were calculated by assuming that the weldment specimen could be represented by a homogeneous, all-weld specimen. This assumption allowed standard equations for the η and γ-factors based on load line measurement to be utilized. The J-integral was computed using the standard formulation [16]:

---

[1] "Standard Method for the Measurement of Fracture Toughness," Draft Standard, Version 14, American Society for Testing and Materials, Philadelphia, PA, September 1994.

$$J = J_{el} + J_{pl} = \frac{K^2}{E'} + \frac{\eta_i}{b_i}\left[\frac{A_{pl(i)} - A_{pl(i-1)}}{B_N}\right]\left[1 - \frac{\gamma_i(a_i - a_{(i-1)})}{b_i}\right] \quad (1)$$

where K = the elastic stress intensity factor,

E' = the plane strain corrected Young's Modulus,

$A_{pl}(i)$ = area under the load vs. plastic load line displacement curve at increment i,

B_N = net specimen thickness,

η_i = the plastic η factor at crack length a_i,

b_i = the remaining ligament at increment i,

W = the specimen width, and

$$\gamma_i = \left[\eta_i - 1 - \frac{b_i}{W}\frac{\frac{d\eta_i}{d(a/W)}}{\eta_i}\right] \quad (2)$$

For the deeply cracked specimens, $\gamma = 1.0$ and $\eta = 2.0$ [16]. However, for $a/W < 0.282$, Sumpter [26] has shown that the following η-factor formulation is valid:

$$\eta = 0.32 + 12\left(\frac{a}{W}\right) - 49.5\left(\frac{a}{W}\right)^2 + 99.8\left(\frac{a}{W}\right)^3 \quad (3)$$

The short crack specimens all failed within $a/W = 0.282$ so Eq. (3) was applied throughout the testing regime. The γ-factor was computed from Eq. (2) using Eq. (3). After the initial data was obtained, the initial and final crack lengths were measured as per ASTM E1152 and the data was shifted by forcing the linear term of a third order polynomial fit of the J-R curve to match the theoretical blunting line, $J = 2\sigma_f \Delta a$, where σ_f was the flow stress for the

homogeneous weld specimen [27].

BASEPLATE AND WELD METAL CHARACTERIZATION

Average tensile properties are summarized in Table 2 for the weld consumables and the base plate steels. The tensile properties are consistent with the nominal properties expected for the weld consumables and baseplate steels. The final percent elongation (e_f) of the Mil-70S and Mil-100S consumables is better than even the baseplate steels. The elongation of the high strength consumable Mil-120S, however, is demonstrably worse. There are small, yet statistically significant differences between σ_{ys} and σ_{ult} for the two Mil-70S welds tested. The three Mil-100S welds possess similar differences. Analysis of variance calculations revealed that the probability that these differences represent actual property variations is 0.95. Differences among the individual weld properties and the average values reported, however, are less than 5% in every case. Only the average weld properties are reported in Table 2.

The mismatch ratio (%Mis) is defined in this research by the following equation:

$$\%\ Mis \equiv \frac{\sigma_{ys}^{weld} - \sigma_{ys}^{base}}{\sigma_{ys}^{base}} \times 100 \qquad (4)$$

where σ_{ys}^{weld} = the all-weld metal yield strength,

and σ_{ys}^{base} = the base metal yield strength.

The mismatch ratio for each baseplate and weld consumable combination is presented in Table 3. This ratio is based on the average tensile properties for the baseplate and weld

consumables presented in Table 2. Similar mismatch ratios were achieved for the HY-80/Mil-70S and HY-100/Mil-100S systems and the HY-80/Mil-100S and HY-100/Mil-120S systems. Therefore, performance comparisons among these systems can be based primarily on the fundamental properties of the weld consumables.

The mean Charpy V-notch energies (CVE) characterizing the transition behavior are represented by the plots in Fig. 4. Curves have been used to indicate data trends and not in an attempt to accurately characterize the ductile to brittle transition curve. Identification of the welds utilized for full transition curve testing is also included in this figure.

These limited Charpy results illustrate the following trends. The lower shelf energies of the Mil-100S and Mil-120S welds are slightly higher than for the Mil-70S weld. The temperature representing the median Charpy energy is the lowest for Mil-120S, slightly higher for Mil-100S, and the highest for Mil-70S. This trend implies that the ductile to brittle transition temperature of these consumables also follows a similar ranking. The biggest apparent differences among the Charpy results are the upper shelf energies and the transition temperature range. Mil-70S and Mil-100S have higher upper shelf energies and much steeper transition ranges.

There also appears to be large differences among the Charpy results from individual weldments. These differences are deceiving in Fig. 4, however, because the variation in the mean (not shown) is large due to the nature of weld metal Charpy testing. This variation was routinely as high as 50% of the mean. Analysis of variance calculations at each test temperature were carried out to determine if differences in the means were statistically meaningful. A 95% confidence limit criteria was used.

The two Mil-70S consumables do possess meaningful differences at 0°C and 20°C as the transition range approaches upper shelf. The mean Charpy results of the six Mil-100S weld consumables are not statistically different at any temperature. The three Mil-120S consumables are similar at the upper and lower shelf, but meaningful differences were found between the GXO and GXM weldments within the transition temperature region. Therefore, there are some toughness differences among similar weld consumables that will be considered when analyzing the crack resistance results. However, the variation among nominally similar consumables is smaller than differences among the consumable types.

RESULTS AND DISCUSSION

Weldment Tensile Performance

The yield strength (σ_{ys}^{s}), ultimate strength (σ_{ult}^{s}), and percent elongation at failure (e_f^{s}) of the undermatched weldment specimens are summarized in Table 4. Average weldment tensile specimen results are reported in this table. The property L_{ht} is the average weld joint height measured on each specimen and D is the specimen diameter (12.7 mm). Results have been normalized with respect to the base metal properties (σ_{ys}^{b}, σ_{ult}^{b}, and e_f^{b}) corresponding to each weldment.

This table reiterates the importance of both mismatch level and constraint (L_{ht}/D) on tensile performance. As the undermatch level increases at a given constraint, the composite yield strength, ultimate strength, and failure ductility can substantially decrease. This is particularly evident between the GXS and GXT specimens with $L_{ht}/D = 0.9$. When mismatch level is constant and weld metal constraint increases, the composite yield and ultimate strength

increase while the composite failure ductility decreases. Failure can actually occur within the baseplate specimen if the constraint is high and the undermatching level is moderate. This phenomenon occurred in both the GXP and GXS specimens with $L_{ht}/D < 1$. In these specimens, however, the composite failure ductility was still significantly less than the baseplate ductility.

Figure 7 illustrates the behavior measured by the baseplate and weld strain gages as well as the composite weldment response measured by the extensometer. It should be noted that the baseplate and weld strain gages generally agreed with the results from the all-weld and baseplate specimens (summarized in Table 2) unless constraint was high ($L_{ht}/D < 1$). Initial weldment specimen yielding (Fig. 7) occurs close to the weld metal yield point regardless of constraint. The effects of constraint appear to be most prominent during a hardening phase after this initial yielding. The degree of this hardening is clearly a function of constraint and mismatch level. After a certain strain (roughly 1% in Fig. 7), the constraint hardening phase ends and the composite response essentially parallels the baseplate flow properties. The constraint hardening trends do somewhat influence the 0.2% offset σ_{ys} measurements reported in Table 4. However, a measure of the stress at roughly 1% strain may provide a more accurate account of the specimen to baseplate (or weld) strength ratio between 1% strain and failure.

Figure 8 compares this testing to earlier measurements [6] on weldments with straight fusion zones oriented perpendicular to the specimen axis. A round specimen geometry was employed [6] as in the current tests. These earlier measurements were for a similar specimen geometry and indicate that weld metal strengthening occurs when $L_{ht}/D < 1$ and is relatively

independent of the amount of undermatching. The amount of undermatching appears only to influence σ_{ult}^{s} in the limit as $L_{ht}/D \rightarrow 0$, which is ideally the baseplate strength.

The current results show that when conventional, beveled weld joint geometries are tested with moderate amounts of undermatch, some contact strengthening occurs at even low constraint levels ($2< L_{ht}/D < 4$). Also, contact strengthening is greater than the earlier measurements at higher constraints ($L_{ht}/D < 1$) and does appear to be a function of the undermatch level. These differences at higher constraint may partially stem from the fact that the current results are plotted in terms of the mean weld joint height, L_{ht}, while the minimum weld joint height may the more influential dimension. However, at lower constraint where the difference between the actual and minimum joint height causes little change in constraint, there still appears to be a strengthening benefit as the joint geometry included angle increases from zero as in the earlier results [6].

However, this apparent increase in strength from beveled joints also degrades the weldment failure ductility (Fig. 8). The ductility of Satoh and Toyoda's specimens approach the all-weld limit by $L_{ht}/D \approx 1$ while the failure ductility measured in the current tests is much lower ($e_f^s/e_f^w = 0.65$) at the same constraint. The increase in ductility as the constraint decreases is also more gradual than in [6] even for specimens with a nominal, -15%, mismatch. Fig. 8 also indicates the strong influence of mismatch on failure ductility: a decrease of over 60% occurred at $L_{ht}/D \approx 0.9$ when the undermatch level was increased from 11% to 36%.

Weldment Cracking Resistance

Baseline Toughness -- The baseline, deep crack, cracking resistance behavior for the three different weld consumables is illustrated in Fig. 9. These results are considered to be the baseline behavior because the L_{gap}/a ratios are all less than 0.8 (Fig. 2) which minimizes the effect of mismatch on the driving force. Further, the specimen constraint is high in the a/W = 0.5 specimens and represents the lower bound R-curve behavior [27].

This figure illustrates that the cracking resistance of the Mil-70S and Mil-100S consumables is much better than the Mil-120S consumable. This confirms the CVE trends in Fig. 4. The R-curve behavior of the 70S and 100S wires are, in fact, very similar although this becomes more apparent in subsequent figures. In the deep crack tests, the 100S weld wire did tend to cleave more which is why the Mil-100S R-curve terminates abruptly. The other curiosity contained within Fig. 9 are the two results for the Mil-120S weld. Deep crack Mil-120S specimens consistently followed one of two paths: either they blunted and then cleaved with little crack growth (upper plot in Fig. 9) or they began tearing almost immediately, continued tearing with relatively little increase in tearing resistance, but did not cleave (lower plot in Fig. 9). Of the five deeply cracked specimens tested, two had behavior representative of the lower plot and three fractured by following the upper path. Research is currently ongoing to explain this curious phenomenon.

Short Crack Effects -- An example of the short crack effect for the undermatched, HY-80 weldment, GXK, is presented in Fig. 10. This figure shows that the tearing resistance increases for the short crack specimen compared to the more deeply cracked specimen. This

trend is well known in homogeneous baseplate specimens [27] and occurs due to loss of crack-tip constraint in the short crack specimen.

Fig. 10 also illustrates two short crack specimens with different L_{gap}/a ratios. The larger L_{gap}/a ratio possesses an apparent increased tearing resistance while the smaller L_{gap}/a ratio closely follows the deep crack behavior. This trend will subsequently be examined more fully, but is used in this figure to illustrate that the short crack effect, while evident, is not large and appears to have less influence on the crack growth resistance than undermatching and weld joint geometry effects. This behavior is similar in the Mil-100S and 120S welds: a short crack effect is present in the R-curve behavior, but it is easily masked by other, more prominent effects.

The short crack tearing resistance for a number of specimens is illustrated in Fig. 11 at two distinct L_{gap}/a ratios. The first plot shows results from specimens with $L_{gap}/a > 2.8$ where mismatching effect should begin to diminish. This plot is similar to Fig. 9 which shows that the cracking resistance of the Mil-70S and 100S consumables are similar and tougher than the Mil-120S consumable. The behavior of the short crack Mil-120S weldments also indicates that the tearing resistance behavior of this consumable is not unique as in the deep crack results.

The lower plot (Fig. 11) is in a regime ($L_{gap}/a \approx 1.3$) where undermatching effects are expected to be large. This figure illustrates a number of important points. First, the difference between the apparent cracking resistance of the Mil-100S and Mil-70S weld wires has decreased compared to $L_{gap}/a > 2.8$ results. Undoubtably this occurs due to the increased crack-tip driving force in the undermatched specimens. However, the Mil-100S and Mil-70S

still have better apparent toughness than the Mil-120S weldments even though the difference has decreased. At no L_{gap}/a ratio was this trend reversed. Another important point that the plot for $L_{gap}/a = 1.3$ indicates is that the effect of undermatch level does not appear to be a primary influence on the J-R behavior in these tests. The mismatch ratio of the GXT specimens is over 3 times greater than the GXR and GXU systems and while the tearing resistance is certainly slightly less, the difference is no greater than at the higher L_{gap}/a ratio and the difference is even less than the variability among the two Mil-100S systems plotted (Fig. 11). The additional specimen constraint due to the applied bending may serve to lessen the influence of mismatch level.

Effect of L_{gap}/a on J-R curves -- The effect of the weld fusion zone width on apparent crack growth resistance behavior is demonstrably illustrated in Fig. 12. This figure illustrates the J-R curves measured for specimens located in the same weldment. This weldment, GXS, had a single-V joint geometry with a nominal root gap of less than 2 mm and a 45° included angle. Three SE(B) specimens were notched in the large gap side of the weldment ($L_{gap}/a = 2.8$) and three were tested with notches in the small gap side of the weldment ($L_{gap}/a = 0.5$). Even though the amount of undermatching is a moderate 11%, the difference in apparent tearing resistance is remarkable, much bigger than is implied in Fig. 2 and in earlier studies [10,11]. Of course the tearing resistance has not actually changed, but two somewhat competing mechanisms are at work which lead to this behavior. Most importantly, the undermatched weld, coupled with a fusion line located relatively close to the crack tip leads to increased deformation (or driving force) at the crack tip. This increased deformation

is not measured as applied J in the experiment because these measurements are based on far-field measurements of load-line and/or crack mouth opening displacement. This driving force increase is only sensed locally at the crack tip and the measurements are insensitive to these effects. If the local J were measured, the two driving force curves should fall more closely together. The second, more subtle, mechanism affecting the J-R curves is crack tip constraint. When the crack tip is near the fusion line in an undermatched weld, more extensive yielding occurs which results in a loss of crack-tip constraint. In baseplate specimens, constraint loss leads to increasing R-curve behavior [27] and a similar effect should be expected here.

The weld fusion zone effect is also illustrated in Fig. 13 which shows a montage of all the HY-100 and Mil-100S weldment systems tested. The trend is unmistakable; as L_{gap}/a increases the apparent R-curve resistance also increases. The results for the overmatched HY-80 and Mil-100S system are also included and show that the "baseline" short crack tearing behavior is consistent with the behavior in the undermatched weldments as $L_{gap}/a \rightarrow 3.5$. This trend remains consistent for the Mil-70S weldments.

A montage of all the Mil-120S testing is presented in Fig. 14. There is no systematic relationship between L_{gap}/a and tearing resistance for these welds. The variability among the behavior for distinct weldment systems overwhelms any mismatch effects which are present, even in greatly overmatched systems. Once again, this behavior confirms the earlier Charpy results presented herein and also experience with the difficulties involved in welding these consumables and obtaining consistent properties.

CONCLUSIONS

This study has examined the effects of weld met mismatching (where the base and weld material flow properties differ) on tensile behavior and crack resistance performance under applied bending loads. The objective was to determine if undermatched welds in high strength steel components have better, or at least adequate, performance compared to an overmatched weldment with the same base material. Weldments with different combinations of base material (HY-80 and HY-100), weld consumable (Mil-70S, Mil-100S, and Mil-120S), and weld joint geometry were manufactured for comparison. Tensile and Charpy characterization of homogeneous base and weld materials indicated that some variation could be expected among different welds with nominally the same consumable. Variations in yield and tensile strength were small, less than 5% of the mean, yet consistent in the Mil-100S and Mil-70S welds. Charpy scatter was much more extensive, although there was so much variability within a single weld that large apparent differences among weldments were not statistically significant. There were statistically significant differences found among Mil-120S welds, however, especially in transition, and near the upper shelf of the two Mil-70S weldment systems. Even with these differences, the Charpy testing indicated that differences among the different consumables was greater than variability within weldments of a single consumable.

Instrumented tensile testing was used to indicate the effects of weld joint height and undermatch on properties of the composite transverse weldment specimens. Yielding initiates near the weld metal yield strength, but hardening can occur soon after and result in higher measured yield and ultimate strengths compared to the weld metal properties. As the amount

of undermatching increases and joint constraint decreases, contact strengthening decreases and the weldment strength approaches that of a homogeneous weld specimen. Contact strengthening still occurs at low constraint in weldments with small amounts of undermatch and beveled joint dimensions. However, failure ductility in these weldments is poor, much worse than for unbeveled weld joint profiles.

Baseline crack resistance to bend loading was measured using short crack (a/W = 0.15) and deep crack (a/W = 0.5) SE(B) specimens having weld joint geometries intended to be minimally influenced by mismatching effects. Mil-100S and Mil-70S were found to have similar tearing resistance curves while the Mil-120S consumable possessed much lower resistance to cracking and also more variability. When weld joint geometries expected to possess large mismatching effects were tested, differences among the consumables' tearing resistance behavior decreased. However, the tearing resistance in the undermatched systems was always greater than the overmatched systems analyzed in this study.

The effect of weld joint geometry on the apparent tearing resistance behavior can be large. As the smaller weld joint height decreases ($L_{gap}/a < 1$), the applied deformation at the crack tip increases and is not accounted for experimentally. Therefore, it appears as if the tearing resistance decreases as L_{gap}/a decreases. This trend is primarily a function of geometry; changes in the level of undermatch by a factor of three did not greatly decrease the J-R curve further. These geometry effects were consistently present in the Mil-100S and 70S systems, but were masked in the Mil-120S welds by the inherent variability of this consumable.

REFERENCES

1. Hartbower, C.E. and Pellini, W.S., "Explosion Bulge Test Studies of the Deformation of Weldments," Welding Journal -- Welding Research Supplement, June 1951, pp. 307s-318s.

2. Hartbower, C.E. and Pellini, W.S., "Investigation of Factors which Determine the Performance of Weldments," Welding Journal -- Welding Research Supplement, October 1951, pp. 499s-511s.

3. Czyryca, E.J, Link, R.E., Wong, R.J., Aylor, D.A., Montemarano, T.W, and Gudas, J.P, "Development and Certification of HSLA-100 Steel for Naval Ship Construction," Naval Engineers Journal, May 1990, pp. 63-91.

4. Denys, R., "Strength and Performance Characteristics of Welded Joints," Mis-Matching of Welds, ESIS 17 (Ed. by K.H. Schwalbe and M. Koçak, Mechanical Engineering Publications, London, 1994, pp. 59-102.

5. Shron, R.Z. and Bakshi, O.A., "The Static Tensile Strength of Welded Joints in Which There is a Soft Interlayer,"Shar. Proiz., No. 9, 1962, pp. 11-14.

6. Satoh, K. and Toyoda, M., "Static Tensile Properties of Welded Joints Including Soft Interlayer," Transactions of the Japan Welding Society, April 1970, pp. 7-12.

7. Satoh, K., and Toyoda, M., "Static Strength of Welded Plates Including Soft Interlayer Under Tension Across a Weld Line," Transactions of the Japan Welding Society, September 1970, pp. 10-17.

8. Satoh, K. and Toyoda, M., "Joint Strength of Heavy Plates with Lower Strength Weld Metal," Welding Journal -- Welding Research Supplement, September 1975, pp. 311s-319s.

9. Patchett, B.M. and Bellow, D.G., "Narrow Gap Welds Using Under Strength Weld Metal," Proceedings of the Second International Conference on Welding and Energy Related Problems, September 1983, pp. 269-278.

10. Kirk, M.T. and Dodds, R.H., "Experimental J Estimation Formulas for Single Edge Notch Bend Specimens Containing Mismatched Welds," Proceedings of the Eleventh International Conference on Offshore Mechanics and Arctic Engineering, American Society of Mechanical Engineers, Vol. III, Part B, 1992, pp. 439-448.

11. Gordon, J.R. and Wang, Y.Y., "The Effect of Weld Metal Mis-Match on Fracture Toughness Testing and Analysis Procedures", Mis-Matching of Welds, ESIS 17, Ed. by K.H. Schwalbe and M. Koçak, Mechanical Engineering Publications, London, 1994, pp. 351-368.

12. Lee, M.M.K. and Luxmoore, A.R., "An Experimental Study of the Elastic-Plastic Deformation of Double 'V' Butt Welds," Journal of Strain Analysis, Vol. 25, No. 4, 1990.

13. Cray, M.J, Luxmoore, A.R. and Sumpter, J.D.G., "The Effect of Weld Metal Mismatch on J and CTOD," Proceedings of the European Symposium on Elastic-Plastic Fracture Mechanics, Freiburg, F.R.G., 1989.

14. Read, D.T. and Petrovski, B.I., "Elastic-Plastic Fracture at Surface Flaws in HSLA Weldments," Proceedings of the Ninth International Conference on Offshore Mechanics and Arctic Engineering, Vol. III, American Society of Mechanical Engineers, New York, NY, 1990, pp. 461-471.

15. Dong, P. and Gordon, J.R., "The Effect of Weld Mismatch on structural Integrity Assessments," presented at the Sixth Annual North American Welding Research Conference, Columbus, OH, November, 1990.

16. ASTM E1152-87, "Standard Test Method for Determining J-R Curves," 1994 Annual Book of ASTM Standards, American Society for Testing and Materials, Philadelphia, PA, 1994, pp. 744-754.

17. MIL-E-23765, Military Specification: Electrodes and Rods - Welding, Bare, Solid, or Alloyed Cored, Low Alloy Steel, 18 August 1987.

18. MIL-S-16216J, Military Specification: Steel Plate, Alloy, Structural, High Yield Strength (HY-80 and HY-100), 10 April 1981.

19. Holsberg, P.W., Gudas, J.P. and Caplan, I.L, "Navy's Welding Research Picks Up Steam," Advanced Materials and Processes, Vol. 7, 1990, pp. 45-49.

20. MIL-STD-1688(SH), Military Standard: Fabrication, Welding, and Inspection of HY-80/100 Submarine Applications, 9 February 1981.

21. ASTM E8-94, "Standard Test Methods for Tension Testing of Metallic Materials," 1994 Annual Book of ASTM Standards, American Society for Testing and Materials, Philadelphia, PA, 1994, pp. 60-80.

22. ASTM E23-94a, "Standard Test Methods for Notched Bar Impact Testing of Metallic Materials," 1994 Annual Book of ASTM Standards, American Society for Testing and Materials, Philadelphia, PA, 1994, pp. 140-160.

23. Kirk, M.T., "A Cyclic Reverse Bending Technique for Fatigue Precracking from Shallow Notches in SE(B) Specimens," Fracture Mechanics: Twenty Second Symposium, Vol. I, ASTM STP-1131, Ed. by H.A. Ernst, A. Saxena and D.L McDowell, American Society for Testing and Materials, Philadelphia, PA, 1992, pp. 859-879.

24. Joyce, J.A., Hackett, E.M. and Roe, C., "Effects of Crack Depth and Mode of Loading on the J-R Curve Behavior of a High-Strength Steel," Fracture Mechanics, ASTM STP 905, American Society for Testing and Materials, Philadelphia, PA, 1986, pp. 741-774.

25. Link, R.E. and Joyce, J.A., "Experimental Investigation of Fracture Toughness Scaling Models," Constraint Effects in Fracture: Theory and Applications, ASTM STP 1244, Ed. by M. Kirk and A. Bakker, American Society for Testing and Materials, Philadelphia, PA, 1994.

26. Sumpter, J.D.G., "J_c Determination for Shallow Notch Welded Bend Specimens," Fatigue and Fracture of Engineering Materials and Structures, Vol. 10, No. 6, 1987, pp. 479-493.

27. Joyce, J.A. and Link, R.E., "Effects of Constraint on Upper Shelf Fracture Toughness," Fracture Mechanics: 26th Volume, ASTM STP 1256, Ed. by W.G. Reuter, J.H. Underwood and J.C. Newman, Jr., American Society for Testing and Materials, Philadelphia, PA, 1995.

TABLE 1--Chemical composition of base and weld metals.

Material	C	Mn	P	S	Si	Ni	Cr	Mo	Va	Ti	Cu	Ar	Sn	An	Zr	Al
HY-80	0.10-0.20	0.10-0.45	0.020	0.002-0.020	0.12-0.38	2.43-3.32	1.29-1.86	0.27-0.63	0.03	0.02	0.25	0.025	0.030	0.025	---	---
HY-100	0.10-0.22	0.10-0.45	0.020	0.002-0.020	0.12-0.38	2.67-3.57	1.29-1.86	0.27-0.63	0.03	0.02	0.25	0.025	0.030	0.025	---	---
Mil-70S-3	0.07-0.19	0.90-1.40	0.025	0.035	0.40-0.70	---	---	---	---	---	---	---	---	---	---	---
Mil-100S-1	0.08	1.25-1.80	0.012	0.008	0.20-0.55	1.40-2.10	0.30	---	0.10	0.10	---	---	---	---	0.10	0.10
Mil-120S-1	0.13	1.40-2.35	0.012	0.008	0.25-0.65	1.00-2.80	0.60	---	0.10	0.10	---	---	---	---	0.10	0.10

TABLE 2--Average base and weld metal tensile properties.

Material	Weldment ID	σ_{ys} (MPa)	σ_{ult} (MPa)	% Elongation in 50 mm
HY-80 Baseplate	GXK	572	703	21
HY-100 Baseplate	GXO	752	848	25
Mil-70S Weld	GXK, GXT	483	600	30
Mil-100S Weld	GXL, GXR, GXU	669	731	29
Mil-120S Weld	GXM	841	889	18

TABLE 3--Mismatch level in weldment systems.

Weldment System	Weldment ID	% Mismatch
HY-80/Mil-70S	GXK	-16
HY-80/Mil-100S	GXL	+17
HY-80/Mil-120S	GXM,GXN	+47
HY-100/Mil-70S	GXT	-36
HY-100/Mil-100S	GXP, GXQ, GXR, GXS, GXU	-11
HY-100/Mil-120S	GXO	+12

TABLE 4--Summary of weldment transverse tensile properties.

Weld ID	% Mis	L_{ht}/D	$\sigma_{ys}^{s}/\sigma_{ys}^{b}$	$\sigma_{ult}^{s}/\sigma_{ult}^{b}$	e_f^{s}/e_f^{b}
GXK	-16	1.7	0.91	0.92	0.61
GXK	-16	3.7	0.88	0.90	0.85
GXP	-11	0.7	0.98	1.00	0.71
GXR	-11	2.3	0.89	0.87	0.49
GXS	-11	0.9	1.00	1.00	0.75
GXS	-11	3.2	0.92	0.89	0.75
GXT	-36	0.9	0.84	0.89	0.30

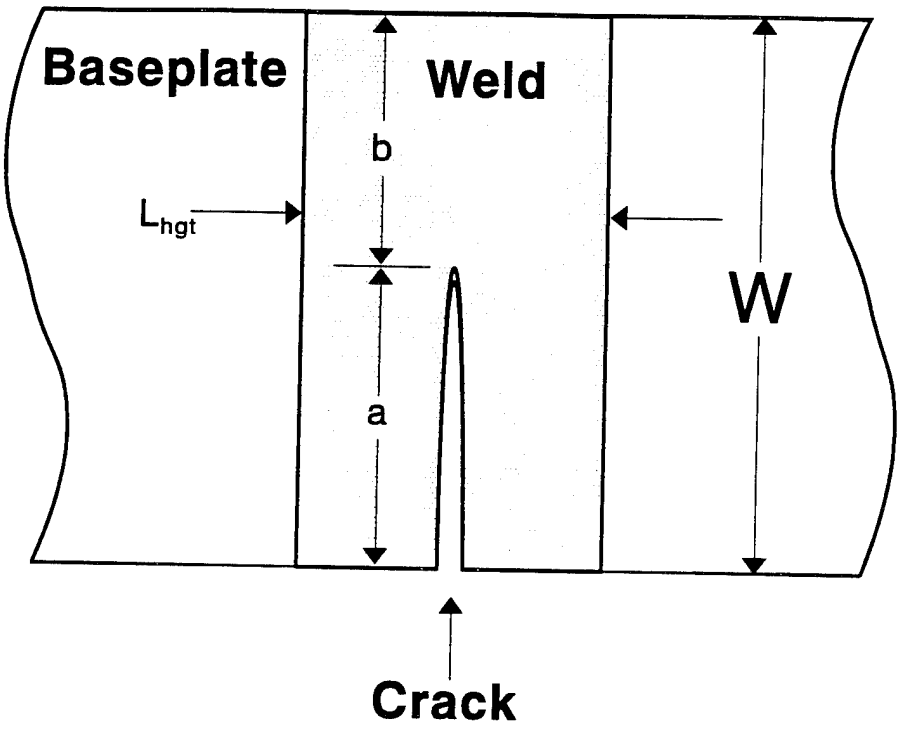

Figure 1--Geometric variables affecting flawed weldment performance.

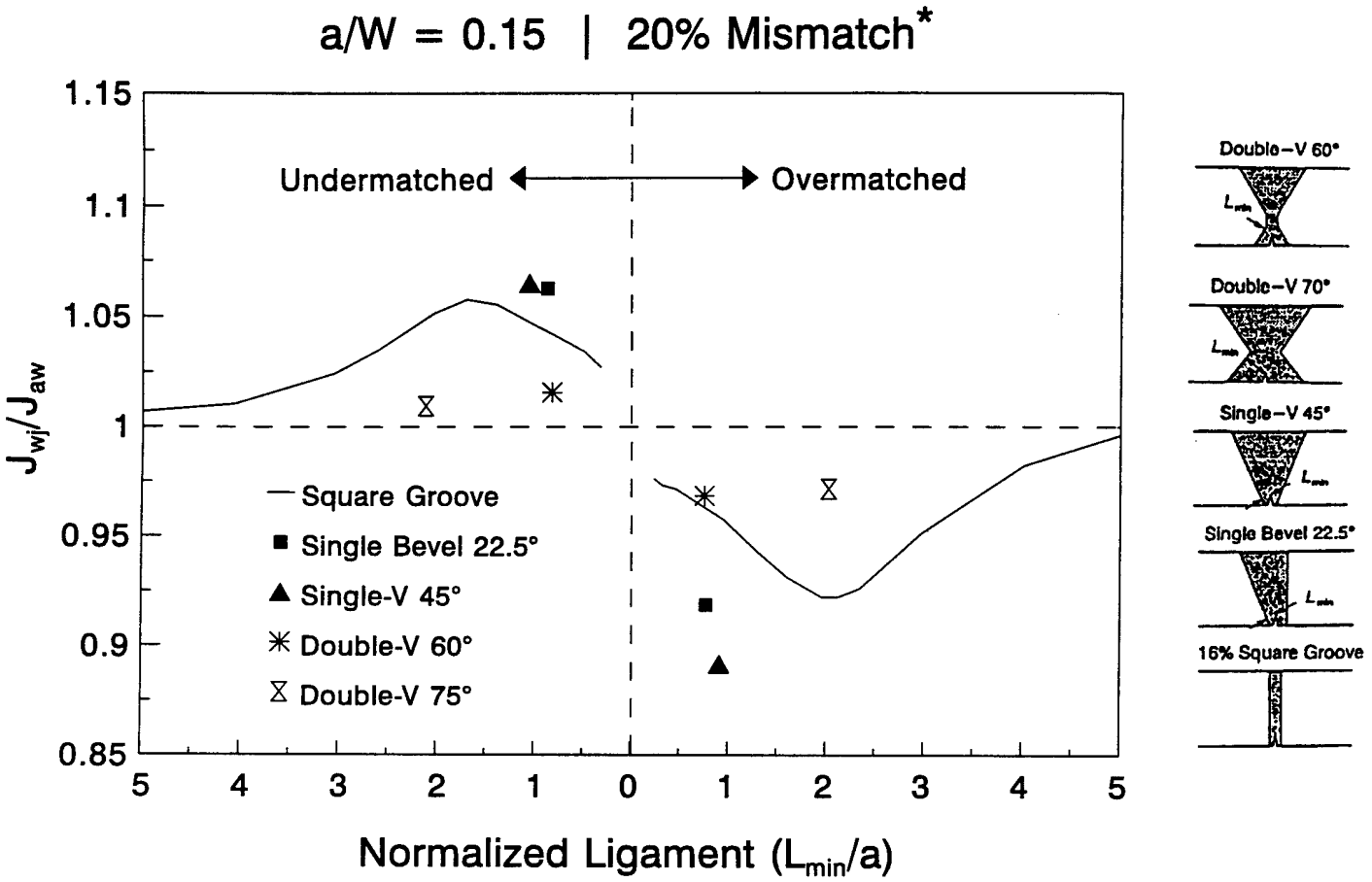

J_{wj} = Weldment Driving Force
J_{aw} = Driving Force in "All-Weld" Specimen

*Fig. taken from [10]

Figure 2--Effect of joint geometry on driving force of mismatched welds.

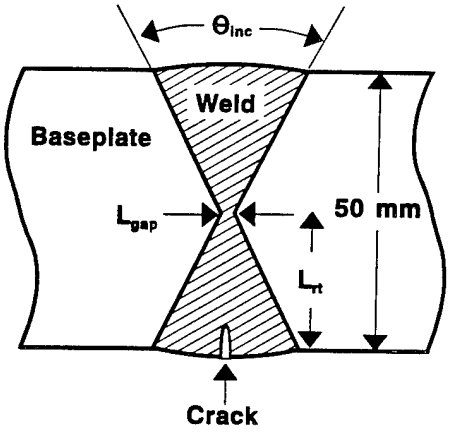

Spec. ID	Base	Weld	Θinc (deg)	Lgap (mm)	Lrt (mm)
GXK	HY-80	70S	60	9.5	12.7
GXL	HY-80	100S	60	9.5	25.4
GXM	HY-80	120S	45	9.5	0
GXN	HY-80	120S	60	3.2	12.7
GXO	HY-100	120S	60	1.6	25.4
GXP	HY-100	100S	60	1.6	25.4
GXQ	HY-100	100S	50	1.6	12.7
GXR	HY-100	100S	50	12.7	12.7
GXS	HY-100	100S	45	0	0
GXT	HY-100	70S	60	1.6	25.4
GXU	HY-100	100S	45	12.7	0

Figure 3--Weld joint geometry and testing matrix.

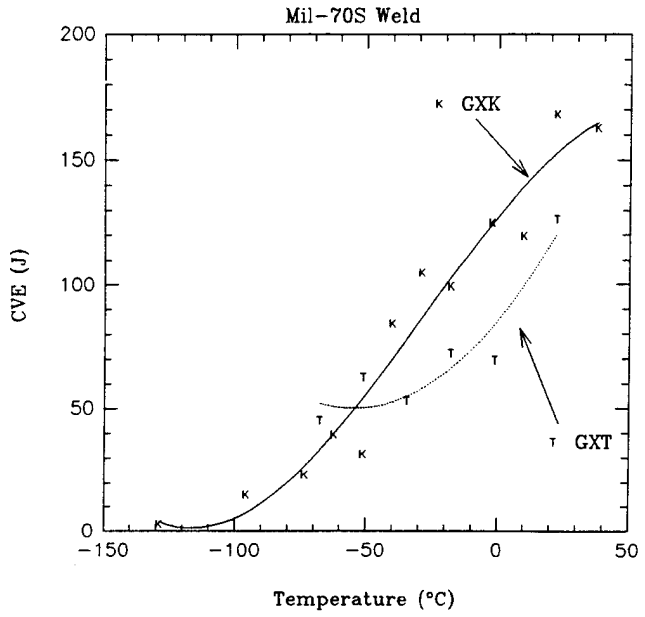

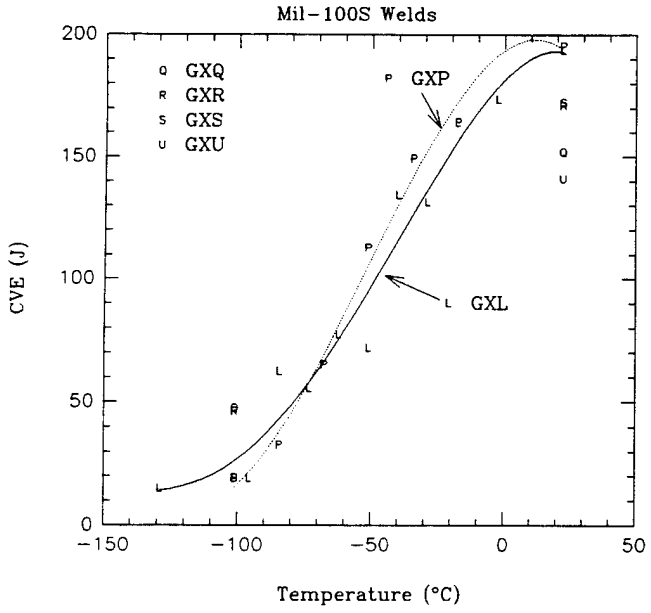

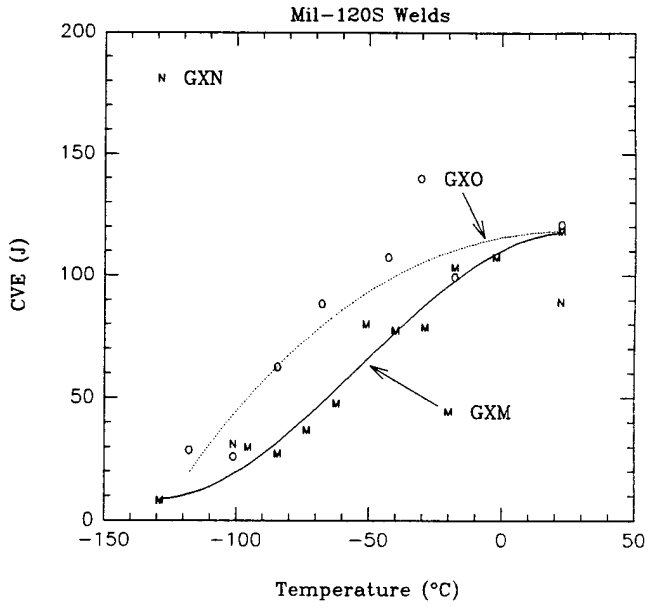

Figure 4--Charpy results for welding consumables tested.

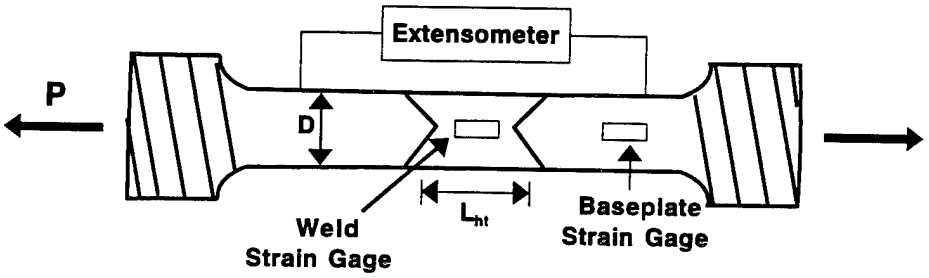

Figure 5--Weldment tensile specimen and instrumentation.

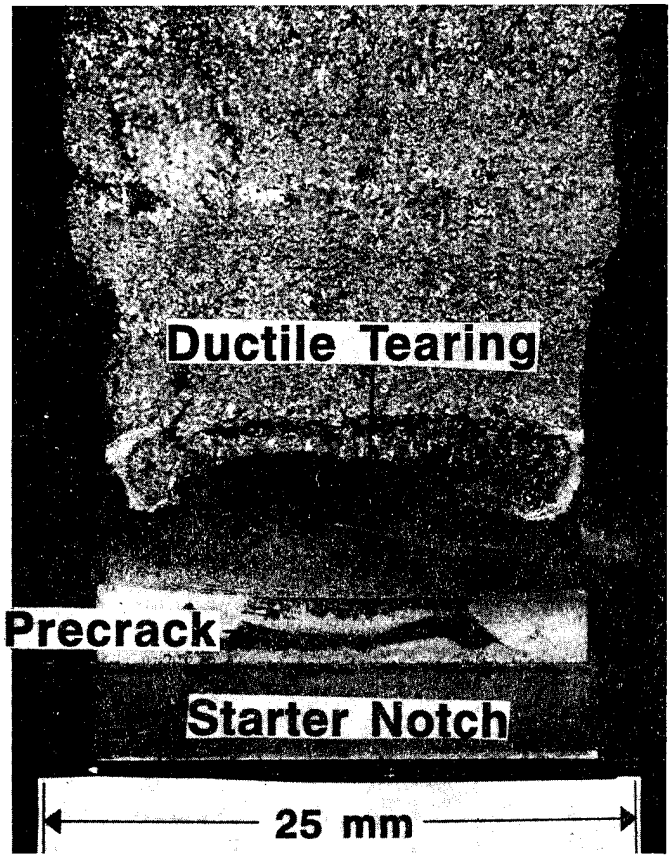

Figure 6--Fracture surface and precrack for undermatched specimen.

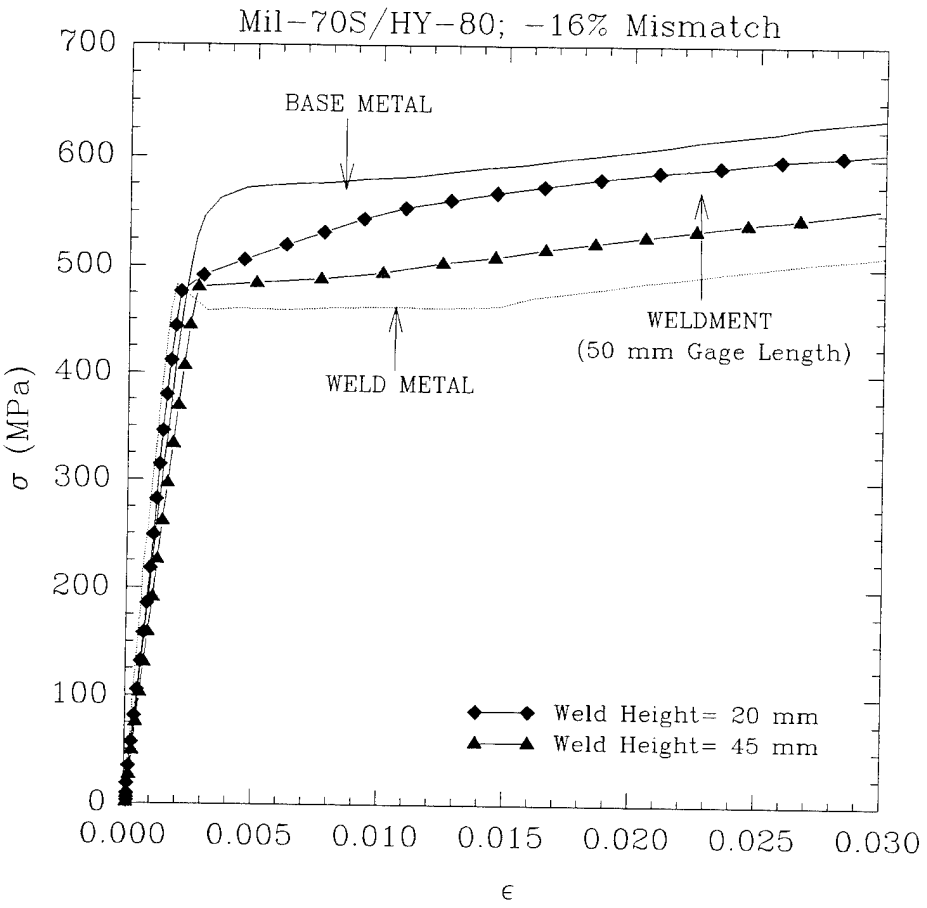

Figure 7--Deformation in unflawed undermatched specimens.

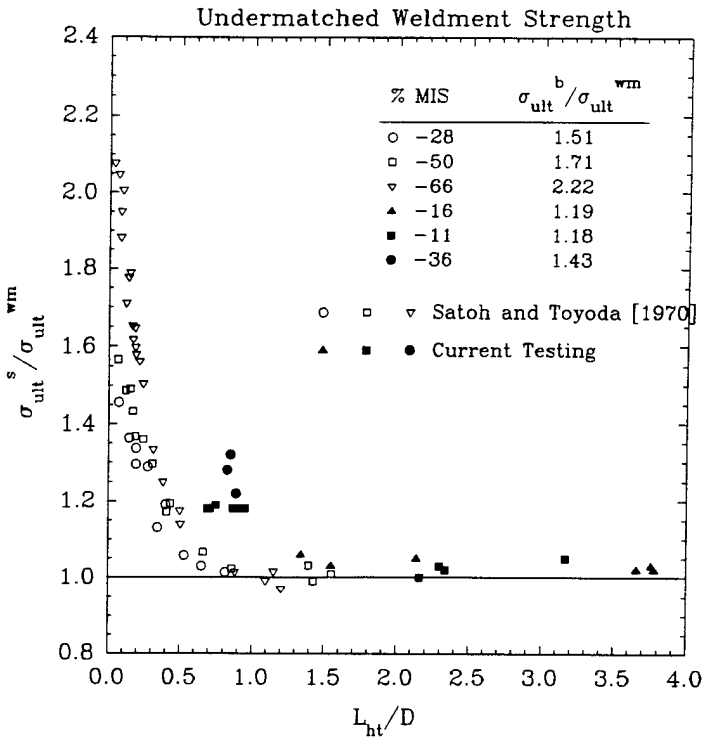

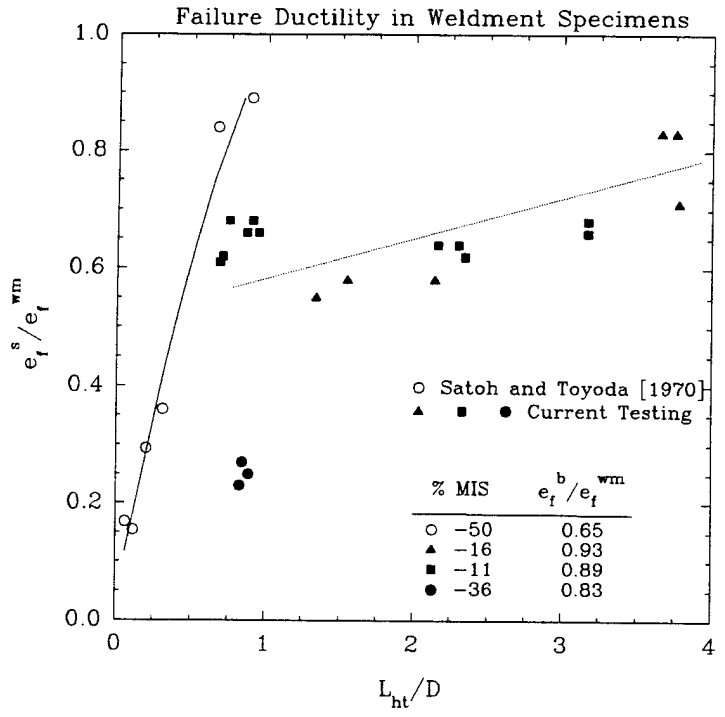

Figure 8--Tensile performance of undermatched welds.

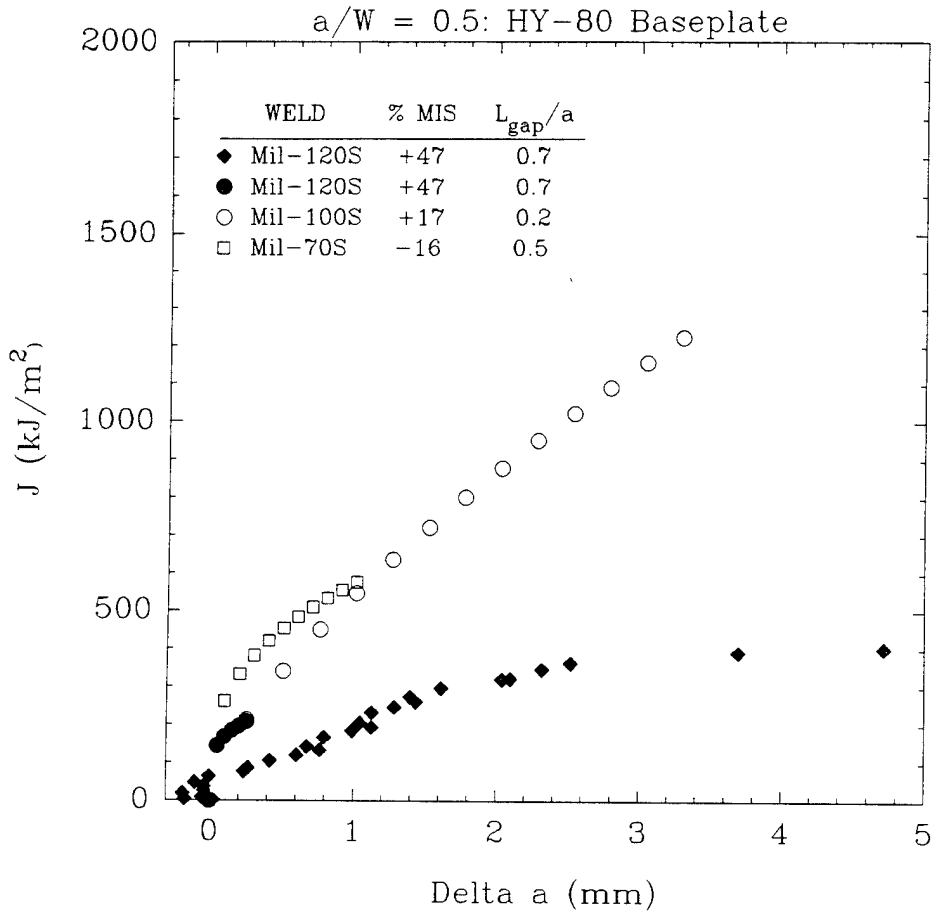

Figure 9--Baseline weld consumable J-R curve behavior.

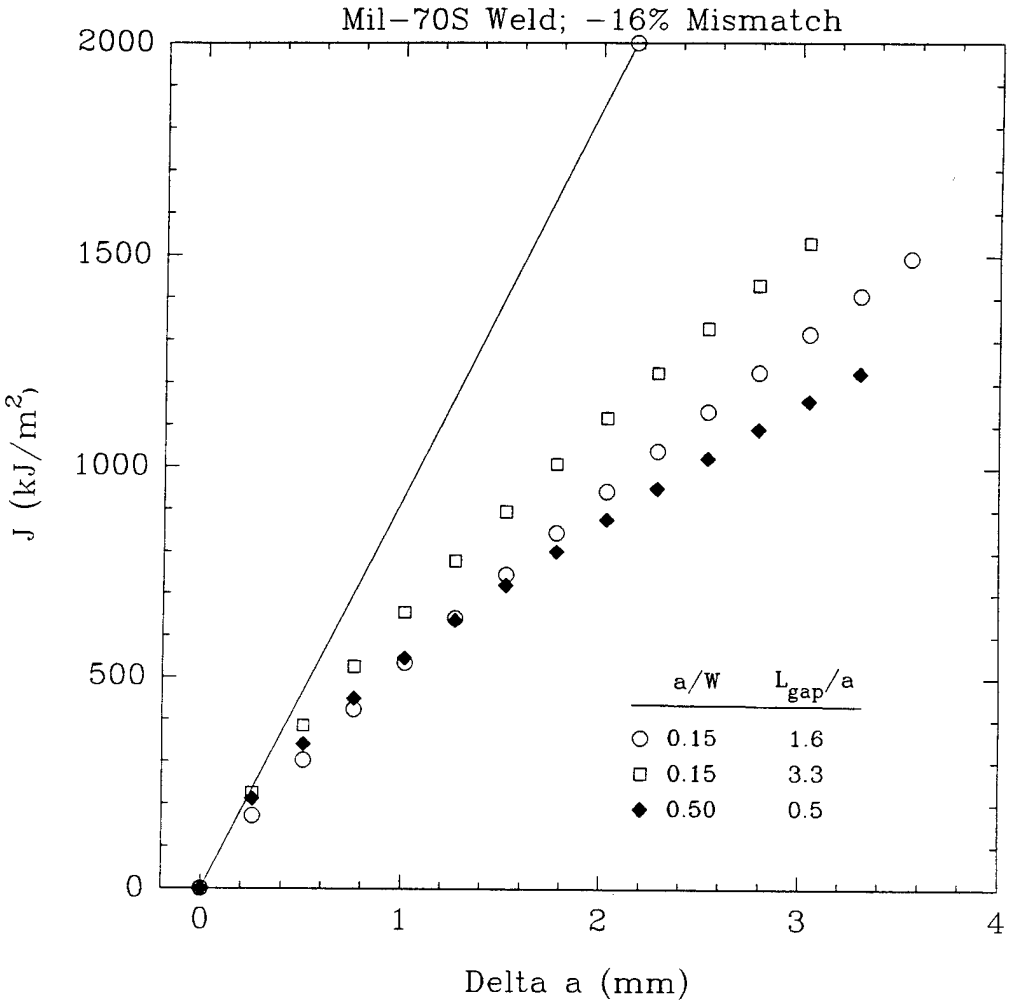

Figure 10--Short crack effect in Mil-70S consumable.

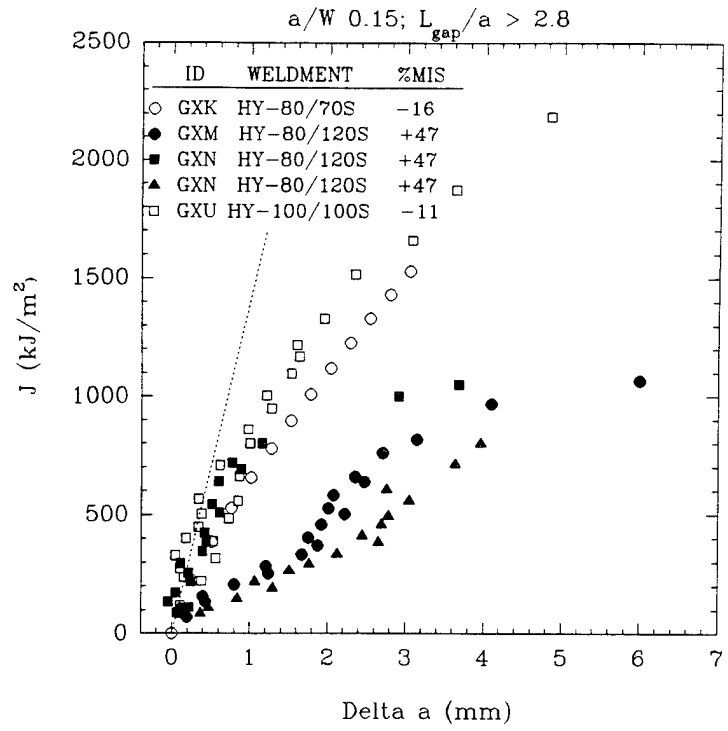

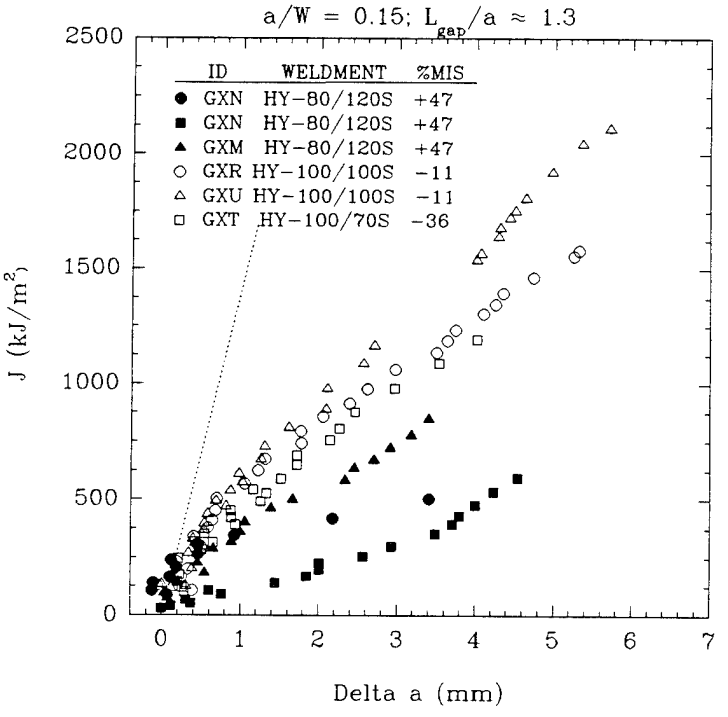

Figure 11--Tearing resistance at fixed L_{gap}/a ratios.

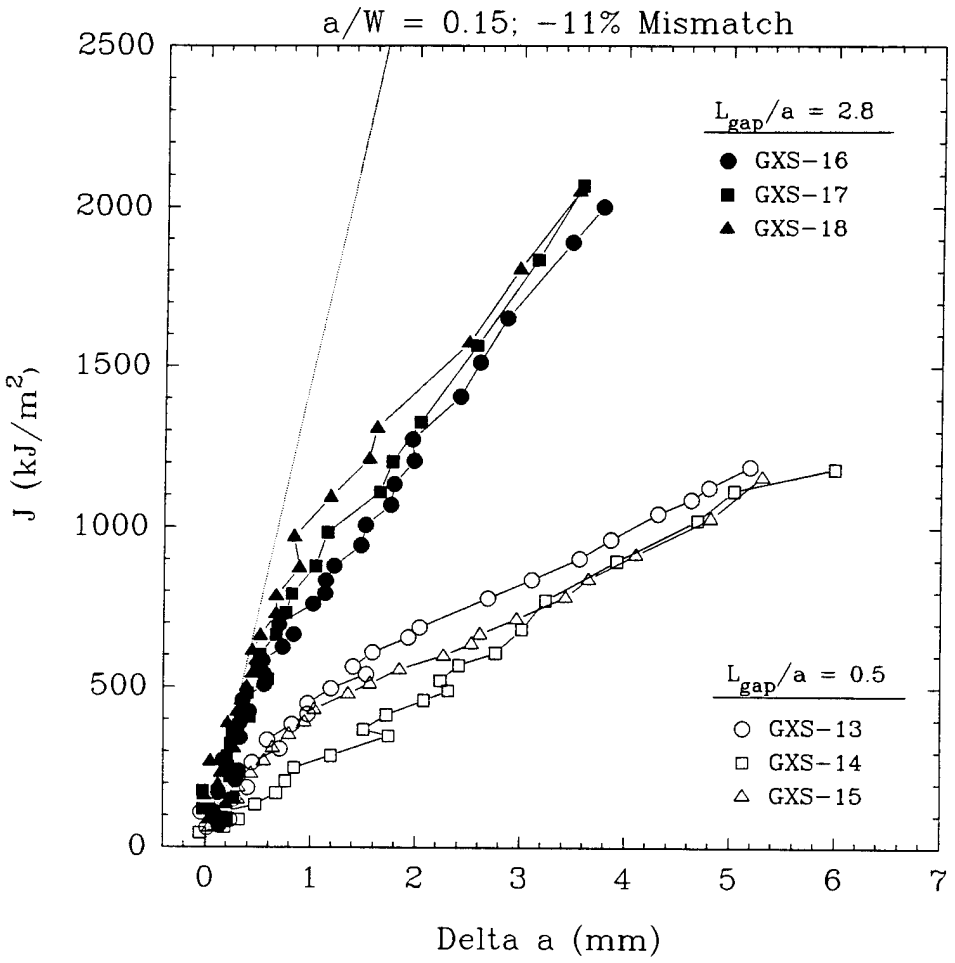

Figure 12--Effect of fusion zone width on tearing resistance.

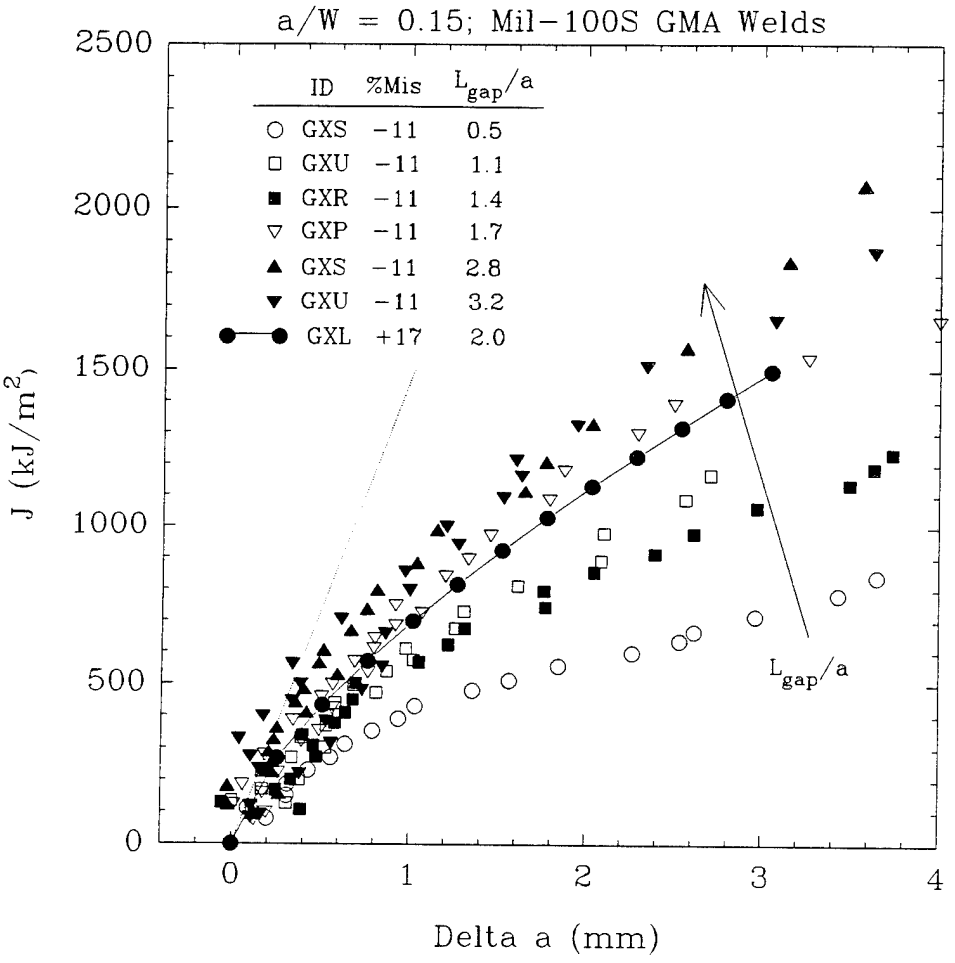

Figure 13--Effects of joint design on tearing resistance in Mil-100S consumable.

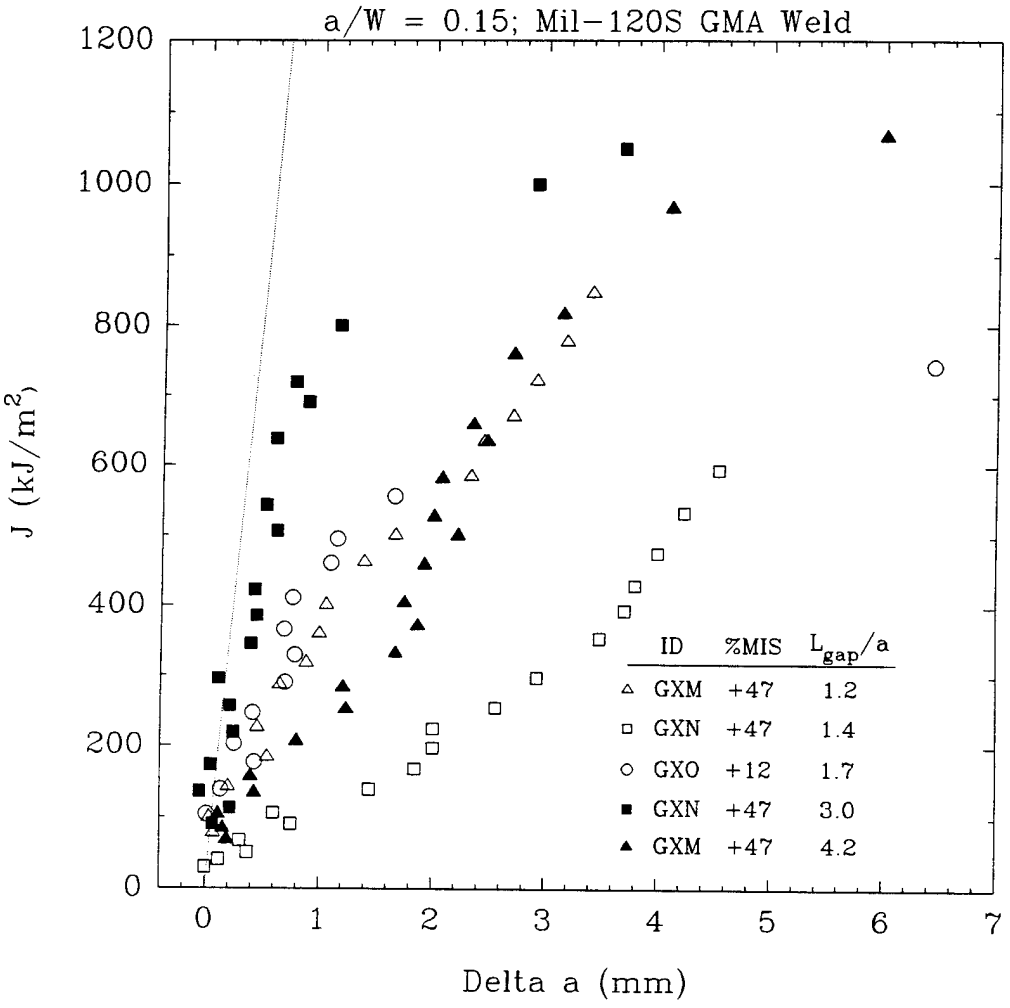

Figure 14--Effect of joint design on tearing resistance of Mil-120S consumable.

DISTRIBUTION LIST

Outside Distribution		Center Distribution	
Copies	Agency	Copies	Code
13	NAVSEA	2	0115 (Caplan)
1	SEA 03M	1	80
1	SEA 03M1	1	60 (Wacker)
1	SEA 03M2 (Null)	1	601 (Morton)
1	SEA 03M2 (Mitchell)	1	602 (Rockwell)
1	SEA 03P1	1	603 (Cavallaro)
1	SEA 03P2	1	604 (Desavage)
1	SEA 03P3	1	605 (Fisch)
1	SEA 03P4 (Nichols)	1	62 (Eichinger)
1	SEA 03P4 (Manuel)	1	623 (Novielli)
1	SEA 08 (Tanner)	1	624 (Hamilton)
1	SEA PMS 350T (Siel)	1	625 (Callahan)
1	SEA PMS 350T1 (Cox)	1	63 (Alig)
1	SEA PMS 393T	1	631 (Ruediger)
		1	64 (Fischer)
2	DTIC	1	65 (Beach)
		3	65.4 (Wiggs)
5	ONR	1	66
1	334 (Barsoum)	1	66.3 (Hay)
1	334 (Rajapakse)	1	67 (Hansen)
1	332 (Sloter)	1	67.1 (Whang)
1	332 (Yoder)	1	68 (Mueller)
1	332 (Sedriks)	1	68.3 (Gray)
1	332 (Vasudaven)	1	69
		5	61 (Holsberg)
4	NRL	1	611 (Palko)
1	6310	1	612 (Aprigliano)
1	6312 (Bayles)	1	613 (Ferrara)
1	6314	5	614 (Montemarano)
1	6316	10	614 (Tregoning)
		1	614 (Czyryca)
1	DDNSWC	1	614 (Juers)
	4140 (Garrett)	1	614 (Roe)
		1	614 (Focht)
		1	614 (Werchniak)
		1	615 (Denale)
		1	615 (Wong)
		1	3421
		1	3422
		2	3431

REPORT DOCUMENTATION PAGE

Form Approved
OMB No. 0704-0188

1. AGENCY USE ONLY (Leave blank)	2. REPORT DATE	3. REPORT TYPE AND DATES COVERED
	July 1995	Final

4. TITLE AND SUBTITLE
Strength and Crack Resistance Behavior of Mismatched Welded Joints

5. FUNDING NUMBERS
WU 94-1-6140-504
WU 95-1-6140-554
ONR: PE62234N, RS34S55

6. AUTHOR(S)
R.L. Tregoning

7. PERFORMING ORGANIZATION NAME(S) AND ADDRESS(ES)
Naval Surface Warfare Center, Carderock Division
Annapolis Detachment
Code 614
Annapolis, MD 21402-5067

8. PERFORMING ORGANIZATION REPORT NUMBER
CDNSWC/TR-61-95-17

9. SPONSORING/MONITORING AGENCY NAME(S) AND ADDRESS(ES)
Carderock Division, Naval Surface Warfare Center
Code 011.5
Bethesda, MD 20084-5000

10. SPONSORING/MONITORING AGENCY REPORT NUMBER

11. SUPPLEMENTARY NOTES

12a. DISTRIBUTION/AVAILABILITY STATEMENT
Approved for public release, July 1995. Distribution is unlimited

12b. DISTRIBUTION CODE
Statement A

13. ABSTRACT

A mismatched welded component exists when the strength of the weld material is different than the strength of the base material. This research has examined the effect of weld joint geometry and the mismatch level on the strength and fracture performance of high strength steel weld components. Eleven different welded systems were constructed with mismatch ranging between -36% to +47% and various weld joint profiles to sculpt fusion zone widths between 2 and 13 mm at the crack tip. Instrumented tensile tests were utilized to characterize weldment strength behavior while single edge notch bend J-R curve testing of short (a/W = 0.15) and deeply (a/W = 0.5) cracked specimens was conducted to measure both baseline weld metal toughness properties and determine the fracture performance of mismatched systems. The results indicate that contact strengthening in unflawed specimens occurs to a greater degree and at lower constraint in conventional undermatched weldments. Flawed undermatched performance is highly dependent on the fusion zone width as well while the degree of mismatching is a secondary effect. As the zone width decreases, the apparent tearing resistance also decreases. The overall performance of undermatched systems, however, can still be better than overmatched systems when the inherent toughness of the overmatching weld metal consumable is poor.

14. SUBJECT TERMS	15. NUMBER OF PAGES
Mismatching, Mismatched Welds, Undermatched Welds, Elastic-Plastic Fracture, J-R Curve, Cracking Resistance, Weld Joint Geometry, Weldment Strength	40
	16. PRICE CODE

17. SECURITY CLASSIFICATION OF REPORT	18. SECURITY CLASSIFICATION OF THIS PAGE	19. SECURITY CLASSIFICATION OF ABSTRACT	20. LIMITATION OF ABSTRACT
Unclassified	Unclassified	Unclassified	SAR